Journal of Sound and Vibration (2001) **246**(3), 491–504
doi:10.1006/jsvi.2001.3649, available online at http://www.idealibrary.com on IDEAL®

ANALYSIS OF PRECESSION VIBRATIONS OF THIN-WALL ELASTIC SHELLS IN COMPOUND ROTATION

V. I. GULYAYEV AND I. L. SOLOVJOV

Department of Mathematics, Ukrainian Transport University, 1, *Suvorov str*., 01010, *Kiev*, *Ukraine*.
E-mail: *gulyayev@mail.kar.net*

AND

P. Z. LUGOVYY

Institute of Mechanics of National Academy of Sciences, 3, *Nesterov str*., 03057, *Kiev*, *Ukraine*

(*Received* 2 *October* 2000, *and in final form* 25 *January* 2001)

This paper is concerned with a numerical study of spinning thin-wall disks, conic and spherical shells whose axes perform additional forced slewing. Position and gyroscopic type inertia forces are taken into account. The technique based on linearization of the shell dynamic equations in the vicinity of the state of simple rotation and use of the transfer matrix method is proposed. It has been found through the numerical calculations that the compound rotation of the elastic thin-wall systems may be a reason for their precession vibrations which may reveal a resonant character under certain conditions. The results of experiments with spherical shells are discussed.

The elaborated approach may be used for numerical simulation of dynamics of thin-wall elastic rotors of engines of aircraft during manoeuvres.

1. INTRODUCTION

There is a distinguishing feature in the technology of aircraft engine turbine production. It is common knowledge that an overwhelming majority of engine failures and emergencies occur within the regimes of an aeroplane's take-off, landings and manoeuvres when its rotors are in a state of compound rotation. Aircraft specialists, having long-standing experience of their operation, know about the possible strange behaviour of engines in compound motion and for this reason they set up the engine resource (reliable longevity) by the number of its take-off and landings. But when investigating the engine thin-wall rotor strength it is usual for designers to concentrate their primary attention on the factors associated with the greatest contribution to the overall stress–strain state of its elements. Among these are the aerodynamic forces, high temperature and inertia forces of simple rotation whose angular velocity may amount up to 20 000–30 000 r.p.m. In doing so, they practically do not take into account the gyroscopic inertia force dynamic action originated from the interplay of the flexible thin-wall rotor spinning motion and the aeroplane slewing motion, considering it to be very small and calculating only resultant gyroscopic moment on the assumption that the rotor is absolutely rigid.

But the opinion about insignificance of the additional internal forces generated by the elastic precession vibration of a flexible thin-wall rotor in compound rotation, though true in the general case, may be fraught with concealed hazards. Firstly, the compound rotation

0022-460X/01/380491 + 14 $35.00/0

is the sole and primary source of generation of genuinely periodical loads, which are acting permanently because the aeroplane axis is in incessant reorientation motion. Even if the vibrations set up by the loads have low intensity, they provoke fatigue damage and conduce to their accumulation. Secondly, the gyroscopic interplay between different motions of elastic thin-wall rotor leads to the generation of the so-called precession vibrations. Contrary to usual vibration which is accompanied by standing wave excitation, when the most dangerous extreme stresses occur only in some isolated spots, the precession vibrations are associated with excitation of progressive waves which travel in the circumferential direction of the structure domain. In this situation, the most hazardous stresses may cover wider areas.

Finally, due to the described interaction of the elastic rotor and aeroplane motions the excitation of their resonant vibration is possible. It seems likely that the facts can help one to clarify the statistical data to the effect that over 90 per cent of all aeroplane engines faults and failures prevail in take-off, landings and manoeuvres.

The reason for the resulting situation connected with ignoring the precession vibrations consists of some specific difficulties of the problem of numerical simulation of the mentioned phenomena. The theoretical difficulties are correlated to the necessity to set up and investigate very complicated problems characterized by particular mechanical and mathematical features. They are the complicated nature of the inertia actions including position and gyroscopic forces experienced by the rotor elements. The position (centrifugal) forces depend on the element position and vary with the element elastic displacement in the system vibrations. The gyroscopic (Coriolis) forces are induced by interaction of rotational and rectilinear motions and depend on the velocity of the element elastic displacements. Besides, there are precession gyroscopic inertia forces generated by interaction of the rotor spinning and compulsory slewing motions in its compound rotation.

The existence of gyroscopic terms in the left-hand side of the differential equations causes a skew-symmetrical matrix of coefficients of the unknown velocities. For this reason, when investigating the rotor free vibrations and analyzing its frequency and mode spectra, double-sized matrices must be used. This is attended by splitting the eigenvalue spectrum and doubling the number of free vibration frequency values and modes. The existence of gyroscopic type terms in the right-hand side of the differential equations is associated with the generation of precession vibrations and a necessity to construct complicated modes of elastic motion. The existence of terms connected with position forces causes one to follow the rotor geometry transformation and to use step-by-step techniques.

Owing to the severe difficulties of the problem under review, it is essentially uninvestigated. Shell vibrations in simple rotation were studied in references [1–4]. Some particular questions of compound rotation of thin-wall structures were investigated in reference [5]. A similar dynamic problem for bladed disks was solved in reference [6].

Considered below are problems of compound rotation of thin-wall elastic disks and conical and spherical shells. It has been found that compound rotation of elastic thin-wall systems is a reason for their precession vibrations which may reveal a resonant character under certain conditions. In these cases not only vibration amplitudes but also the total elastic moment acting on the system supports begin to increase very quickly. The results of experiments are discussed too.

2. INERTIA FORCES CALCULATION

To determine the inertia forces acting on an elastic system in compound rotation consider a model of a shell rotor (Figure 1). The shell butt-end is connected to a rigid foundation

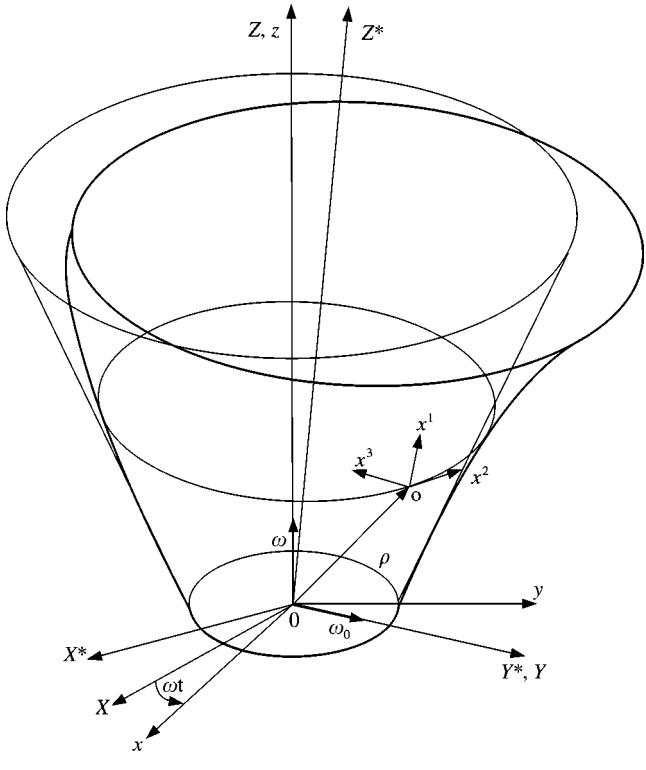

Figure 1. The shell design scheme: ——, initial undeformed state; ▬▬, state of precession vibration.

spinning with a constant angular velocity $\boldsymbol{\omega}$ relative to the shell axis which in its turn is slewing with constant velocity vector $\boldsymbol{\omega}_0$ around the axis perpendicular to $\boldsymbol{\omega}$. To describe the inertia forces incited by the rotor compound rotation, introduce the following right reference frames: $OX^*Y^*Z^*$ is the inertial co-ordinate system with the origin O fixed at the support contour centre and axis OY^* being collinear with the vector $\boldsymbol{\omega}_0$; $Oxyz$—the co-ordinate system fixed to the rotating foundation; $OXYZ$—the slewing co-ordinate system whose axis OY coincides with the axis OY^* and axis OZ is in line with the Oz-axis. In the rotor shell middle surface the local curvilinear orthogonal co-ordinate system $ox^1x^2x^3$ is built whose co-ordinate line x^1 is disposed in the generatrix section, x^2 is directed in the circumferential sense, x^3 is oriented along the internal normal to the shell surface.

The following co-ordinate bases are constructed: the basis $\mathbf{i}^*$, $\mathbf{j}^*$, $\mathbf{k}^*$ in the inertial reference frame OX^*Y^*Z; $\mathbf{i}_1$, $\mathbf{j}_1$, $\mathbf{k}_1$ in the $OXYZ$ reference frame and $\mathbf{i}$, $\mathbf{j}$, $\mathbf{k}$ in the system $Oxyz$. The vectors $\mathbf{e}_1$, $\mathbf{e}_2$, $\mathbf{e}_3$ of the primary basis are directed along the tangents to the shell co-ordinate lines. Vectors of the mutual basis conjugate to the primary one are determined by the correlations

$$\mathbf{e}^i = a^{ij}\mathbf{e}_j \quad (i = 1, 2), \qquad \mathbf{e}^3 = \mathbf{e}_3.$$

Inasmuch as in the case considered only inertia forces are separated for the rotor elastic vibration investigation, their intensity is calculated as follows:

$$\mathbf{p} = -\gamma h\mathbf{a}. \tag{1}$$

Here h is the thickness of a shell element; γ its material density; $\mathbf{a}$ the element absolute acceleration vector calculated with the help of the formula [7]

$$\mathbf{a} = \mathbf{a}_e + \mathbf{a}_r + \mathbf{a}_c, \tag{2}$$

where $\mathbf{a}_e$ is the element bulk acceleration vector; $\mathbf{a}_r$ the element relative acceleration; $\mathbf{a}_c$ its complementary acceleration.

The absolute acceleration (2) components are calculated with the help of the formulas

$$\mathbf{a}_e = \boldsymbol{\varepsilon} \times \boldsymbol{\varrho} + \boldsymbol{\Omega} \times (\boldsymbol{\Omega} \times \boldsymbol{\varrho}), \qquad \mathbf{a}_c = 2\boldsymbol{\Omega} \times \frac{\mathrm{d}\boldsymbol{\varrho}}{\mathrm{d}t}, \qquad \mathbf{a}_r = \frac{\mathrm{d}^2\boldsymbol{\varrho}}{\mathrm{d}t^2}. \tag{3}$$

Here $\boldsymbol{\Omega} = \boldsymbol{\omega} + \boldsymbol{\omega}_0$ is the reference frame $0xyz$ absolute angular velocity vector, $\boldsymbol{\varepsilon} = \boldsymbol{\omega}_0 \times \boldsymbol{\omega}$ its absolute angular acceleration vector, $\boldsymbol{\varrho} = \mathbf{R} + \mathbf{u}$ the deformed shell element position vector in the reference frame $Oxyz$, $\mathbf{R}$ the same vector for the nondeformed shell, and $\mathbf{u}$ the vector of the element elastic displacement. The kinetical parameters of the platform translatory motion are neglected.

It is convenient to construct the vectors $\mathbf{a}_e$ and $\mathbf{a}_c$ in the basis $\mathbf{i}$, $\mathbf{j}$, $\mathbf{k}$ of the co-ordinate system $0xyz$. As a consequence of vector operation fulfilment in equation (3), considering $\omega \gg \omega_0$, ignoring ω_0^2 and after omission of the intermediate transformations, the acceleration vectors in this basis may be represented as follows:

$$\begin{aligned}
\mathbf{a}_e &= \mathbf{i}[-\omega^2(r\cos x^2 + u_1 \sin\varphi \cos x^2/\sqrt{a_{11}} - u_2 \sin x^2/\sqrt{a_{22}} - u_3 \cos\varphi \cos x^2)] \\
&\quad + \mathbf{j}[-\omega^2(r\sin x^2 + u_1 \sin\varphi \sin x^2/\sqrt{a_{11}} + u_2 \cos x^2/\sqrt{a_{22}} - u_3 \cos\varphi \sin x^2)] \\
&\quad + \mathbf{k} 2r\omega_0\omega \sin(\omega t + x^2), \\
\mathbf{a}_c &= \mathbf{i}[2\omega(-\dot{u}_1 \sin\varphi \sin x^2/\sqrt{a_{11}} - \dot{u}_2 \cos x^2/\sqrt{a_{22}} + \dot{u}_3 \cos\varphi \sin x^2)] \\
&\quad + \mathbf{j}[2\omega(\dot{u}_1 \sin\varphi \cos x^2/\sqrt{a_{11}} - \dot{u}_2 \sin x^2/\sqrt{a_{22}} - \dot{u}_3 \cos\varphi\, x^2)] + \mathbf{k}\cdot 0, \\
\mathbf{a}_r &= \partial^2\mathbf{u}/\partial t^2,
\end{aligned}$$

where u_1, u_2, u_3 are the contravariant components of the vector $\mathbf{u}$, $\dot{u}_1, \dot{u}_2, \dot{u}_3$ the appropriate velocity components, a_{11}, a_{22} the parameters of the first quadratic form in the shell surface, r the distance between the considered element and the axis of spinning, $\varphi = \varphi_0 + \vartheta_1^*$, φ_0 the angle of inclination of the shell generatrix tangent to its axis for the nondeformed shell, and ϑ_1^* the corresponding angle of the element elastic slewing.

The basal vectors of the movable co-ordinate system $0xyz$ and primary local system are connected with the correlations

$$\begin{aligned}
\mathbf{i} &= \cos x^2 \sin\varphi/\sqrt{a_{11}} \cdot \mathbf{e}_1 - \sin x^2/\sqrt{a_{22}} \cdot \mathbf{e}_2 - \cos\, x^2 \cos\varphi \cdot \mathbf{e}_3, \\
\mathbf{j} &= \sin x^2 \sin\varphi/\sqrt{a_{11}} \cdot \mathbf{e}_1 - \cos x^2/\sqrt{a_{22}} \cdot \mathbf{e}_2 - \sin\, x^2 \cos\varphi \cdot \mathbf{e}_3, \\
\mathbf{k} &= \cos\varphi/\sqrt{a_{11}} \cdot \mathbf{e}_1 + \sin\varphi \cdot \mathbf{e}_3.
\end{aligned}$$

Taking into account these relationships, the contravariant components of the acceleration vectors may be represented in the local basis as follows:

$$\begin{aligned}
a_e^1 &= -\omega^2 r \sin\varphi/\sqrt{a_{11}} + 2\omega_0\omega r \sin(\omega t + x^2)\cos\varphi/\sqrt{a_{11}} - \omega^2 u_1 \sin^2\varphi/a_{11} \\
&\quad + \omega^2 u_3 \sin\varphi \cos\varphi/\sqrt{a_{11}},
\end{aligned}$$

$$a_e^2 = -\omega^2 u_2/a_{22},$$

$$a_e^3 = \omega^2 r\cos\varphi + 2\omega_0\omega r\sin(\omega t + x^2)\sin\varphi + \omega^2(u_1\sin\varphi/\sqrt{a_{11}} - u_3\cos\varphi)\cos\varphi,$$

$$a_c^1 = -2\omega\dot{u}_2\sin\varphi/\sqrt{a_{11}a_{22}},$$

$$a_c^2 = -2\omega\dot{u}_1\sin\varphi/\sqrt{a_{11}a_{22}} - 2\omega\dot{u}_3\cos\varphi/\sqrt{a_{22}},$$

$$a_c^3 = 2\omega\dot{u}_2\cos\varphi/\sqrt{a_{22}},$$

$$a_r^1 = \ddot{u}_1/a_{11}, \qquad a_r^2 = \ddot{u}_2/a_{22}, \qquad a_r^3 = \ddot{u}_3. \tag{4}$$

The corresponding force expressions based on equations (1) and (4) are inserted into the left- and right-hand side of constitutive equations of the theory of shells. They contain summands depending on displacements, their velocities and accelerations and the phase function $(\omega t + x^2)$ as well. For this reason, it is not only the generation of running loads that is connected with the action of the inertia forces initiated by the compound rotation, but also the structural modification of the constitutive equations left-hand side, including gyroscopic terms. It is known [7] that the gyroscopic forces power equals zero, but they essentially influence on the system motion modes.

3. CONSTITUTIVE EQUATIONS

For the considered problem to be solved the following simplifying assumptions are used. In the rotor dynamics only elastic strains take place and the correlations between stresses and strains are reckoned to be linear. The angular velocity ω is comparatively high so the correlations between strains and displacements at simple spinning are non-linear. Damping forces are not taken into consideration and the elastic gyroscopic system is assumed to be conservative.

With the assumptions being made, the equations of dynamic equilibrium of a rotor shell element in the above-introduced reference frame $Oxyz$ may be represented in the form

$$\mathbf{V}_\alpha\mathbf{T}^\alpha + \mathbf{p} = 0,\ \mathbf{V}_\alpha\mathbf{M}^\alpha + (\mathbf{e}^\alpha\times\mathbf{T}^\alpha) = 0 \quad (\alpha = 1, 2), \tag{5}$$

where $\mathbf{T}^\alpha$ is the vector of internal forces in the shell, $\mathbf{M}^\alpha$ the vector of internal moments, $\mathbf{V}_\alpha$ the symbol of the covariant derivative, and $\mathbf{p}$ the vector of the external distributed forces intensity.

Reduced to the scalar form, the first equation yields

$$\frac{\partial T^{11}}{\partial x^1} + \frac{\partial T^{12}}{\partial x^2} + (2\Gamma_{11}^1 + \Gamma_{21}^2)T^{11} + \Gamma_{22}^1 T^{22} - b_1^1 T^{13} + p^1 = 0,$$

$$\frac{\partial T^{12}}{\partial x^1} + \frac{\partial T^{22}}{\partial x^2} + (3\Gamma_{12}^2 + \Gamma_{11}^1)T^{12} - b_2^2 T^{23} + p^2 = 0, \tag{6}$$

$$\frac{\partial T^{13}}{\partial x^1} + \frac{\partial T^{23}}{\partial x^2} + (\Gamma_{12}^2 + \Gamma_{11}^1)T^{13} + b_{11}T^{11} + b_{22}T^{22} + p^3 = 0.$$

Here Γ^i_{ik} is the Cristoffel symbol, and b^j_i, b_{ij} the parameters of the second quadratic form. The shear forces T^{13}, T^{23} are determined with the help of the system (5) second equation as

$$T^{13} = \frac{\partial M^{11}}{\partial x^1} + \frac{\partial M^{12}}{\partial x^2} + (2\Gamma^1_{11} + \Gamma^2_{21})M^{11} + \Gamma^1_{22}M^{22},$$

$$T^{23} = \frac{\partial M^{12}}{\partial x^1} + \frac{\partial M^{22}}{\partial x^2} + (3\Gamma^2_{12} + \Gamma^1_{11})M^{12}. \tag{7}$$

The contravariant components of the internal forces T^{ij} and moments M^{ij} may be expressed through the covariant components of the strains ε_{ij} and curvature increments μ_{ij}:

$$T^{ij} = \frac{Eh}{1-\nu^2}\,\varepsilon_{\alpha\beta}\,[\nu a^{ij}a^{\alpha\beta} + (1-\nu)a^{i\alpha}\,a^{j\beta}],$$

$$M^{ij} = \frac{Eh^3}{12(1-\nu^2)}\,\mu_{\alpha\beta}\,[\nu a^{ij}a^{\alpha\beta} + (1-\nu)a^{i\alpha}\,a^{j\beta}] \quad (i,j,\alpha,\beta = 1,2). \tag{8}$$

Here E, ν are the shell material modulus of elasticity and Poisson's ratio.

The functions ε_{ij}, μ_{ij} are expressed through the components u_1, u_2, u_3 of the displacement vector $\mathbf{u}$ and angles ϑ_i of the cross-section turn:

$$\varepsilon_{ij} = \frac{1}{2}\left(\frac{\partial \mathbf{u}}{\partial x^j}\cdot\mathbf{e}_i + \frac{\partial \mathbf{u}}{\partial x_i}\cdot\mathbf{e}_j + \vartheta_i\,\vartheta_j\right),$$

$$\mu_{ij} = \frac{1}{2}\left(\frac{1}{c_{ik}}\frac{\partial \boldsymbol{\Omega}_1}{\partial x^j}\cdot\mathbf{e}^k + \frac{\mathbf{1}}{c_{jk}}\frac{\partial \boldsymbol{\Omega}_1}{\partial x^i}\cdot\mathbf{e}^k\right) \quad (i,j,k = 1,2), \tag{9}$$

$$\boldsymbol{\Omega}_1 = c^{ij}\vartheta_i\mathbf{e}_j, \qquad \vartheta_i = -\left(\frac{\partial \mathbf{u}}{\partial x^i}\right)\mathbf{e}_3.$$

The scalar form of the equalities is as follows:

$$\varepsilon_{11} = \frac{\partial u_1}{\partial x^1} - \Gamma^1_{11}u_1 - b_{11}u_3 + \frac{1}{2}\,\vartheta_1^2,$$

$$\varepsilon_{22} = \frac{\partial u_2}{\partial x^2} - \Gamma^1_{22}u_1 - b_{22}u_3 + \frac{1}{2}\,\vartheta_2^2,$$

$$\varepsilon_{12} = \frac{1}{2}\left(\frac{\partial u_2}{\partial x^1} + \frac{\partial u_1}{\partial x^2} - 2\Gamma^2_{12}u_2 + \vartheta_1\vartheta_2\right), \tag{10}$$

$$\mu_{11} = \frac{\partial \vartheta_1}{\partial x^1} - \Gamma^1_{11}\vartheta_1, \quad \mu_{22} = \frac{\partial \vartheta_2}{\partial x^2} - \Gamma^1_{22}\vartheta_1,$$

$$\mu_{12} = \frac{1}{2}\left(\frac{\partial \vartheta_2}{\partial x^1} + \frac{\partial \vartheta_1}{\partial x^2} - 2\Gamma^2_{12}\vartheta_2\right),$$

$$\vartheta_1 = -\frac{\partial u_3}{\partial x^1} - b^1_1 u_1, \qquad \vartheta_2 = -\frac{\partial u_3}{\partial x^2} - b^2_2 u_2.$$

Allowance for the variations of parameters b_i^i, b_{ii} is carried out by the use of the equalities

$$\Delta b_i^i = -a^{ii}\Delta\mu_{ii}, \qquad \Delta b_{ii} = -\Delta\mu_{ii}. \tag{11}$$

After corresponding substitutions of inertial forces (4) and expressions (7) into (6) the first group of dynamic equilibrium equations (5) takes the form

$$\begin{aligned}
&\frac{\partial T^{11}}{\partial x^1} + \frac{\partial T^{12}}{\partial x^2} + (2\Gamma_{11}^1 + \Gamma_{21}^2)T^{11} + \Gamma_{22}^1 T^{22} - b_1^1 T^{13} \\
&\quad = \gamma h\Bigg[-\omega^2 \frac{r}{\sqrt{a_{11}}}\sin\varphi + 2\omega_0\omega\frac{r}{\sqrt{a_{11}}}\sin(\omega t + x^2)\cos\varphi - \omega^2\frac{u_1}{a_{11}}\sin^2\varphi \\
&\qquad + \omega^2\frac{u_3}{\sqrt{a_{11}}}\sin\varphi\cos\varphi - 2\omega\frac{\dot{u}_2}{\sqrt{a_{11}a_{22}}}\sin\varphi + \frac{\ddot{u}_1}{a_{11}}\Bigg], \\
&\frac{\partial T^{12}}{\partial x^1} + \frac{\partial T^{22}}{\partial x^2} + (3\Gamma_{12}^2 + \Gamma_{11}^1)T^{12} - b_2^2 T^{23} \\
&\quad = \gamma h\Bigg(-\omega^2\frac{u_2}{a_{22}} + 2\omega\frac{\dot{u}_1}{\sqrt{a_{11}a_{22}}}\sin\varphi - 2\omega\frac{\dot{u}_3}{\sqrt{a_{22}}}\cos\varphi + \frac{\ddot{u}_2}{a_{22}}\Bigg), \\
&\frac{\partial T^{13}}{\partial x^1} + \frac{\partial T^{23}}{\partial x^2} + (\Gamma_{12}^2 + \Gamma_{11}^1)T^{13} + b_{11}T^{11} + b_{22}T^{22} \\
&\quad = \gamma h\Bigg[\omega^2 r\cos\varphi + 2\omega_0\omega r\sin(\omega t + x^2)\sin\varphi + \omega^2\frac{u_1}{\sqrt{a_{11}}}\cos\varphi\sin\varphi \\
&\qquad - \omega^2 u_3\cos^2\varphi + 2\omega\frac{\dot{u}_2}{\sqrt{a_{22}}}\cos\varphi + \ddot{u}_3\Bigg].
\end{aligned} \tag{12}$$

These equations and correlations (8)–(11) are the constitutive system of geometrically non-linear differential equations of the dynamic behaviour of a thin shell in compound rotation.

In modelling the rotor motion it is assumed that $\omega \gg \omega_0$. This allows one to select two states in the shell overall motion. In the first state the shell performs simple rotation with the angular velocity ω; it is stressed by stationary axisymmetrical centrifugal inertia forces and does not vibrate. In the second one, occurring in the slewing elastic system, additional gyroscopic periodical inertia forces are generated, which excite small precession vibrations with the frequency ω, processing relative to the initial statically stressed state. The condition $\omega \gg \omega_0$ allows one to study the states in turn, using the solution of the first state equations for calculation of coefficients of equations of the rotor vibration in the second state.

To investigate the simple spinning of the rotor, system (12) is used after discarding the terms containing ω_0 and time derivatives and taking into consideration the rotor axial symmetry.

The equations of the rotor precession vibrations are constructed via the correlations (12), linearized in the vicinity of the simple rotation state [8]. After additional transformations they acquire the form

$$\frac{\partial \Delta T^{11}}{\partial x^1} + \frac{\partial \Delta T^{12}}{\partial x^2} + (2\Gamma_{11}^1 + \Gamma_{21}^2)\Delta T^{11} + \Gamma_{22}^1\Delta T^{22} - b_1^1\Delta T^{13}$$

$$= \gamma h\Bigg[-\omega^2 \frac{r}{a_{11}} \cos\varphi \Delta\vartheta_1 + 2\omega_0\omega \frac{r}{\sqrt{a_{11}}} \sin(\omega t + x^2)\cos\varphi - \omega^2 \frac{\Delta u_1}{a_{11}} \sin^2\varphi$$

$$+ \omega^2 \frac{\Delta u_3}{\sqrt{a_{11}}} \sin\varphi\cos\varphi - 2\omega \frac{\Delta \dot{u}_2}{\sqrt{a_{11}a_{22}}} \sin\varphi + \frac{\Delta \ddot{u}_1}{a_{11}} \Bigg],$$

$$\frac{\partial \Delta T^{12}}{\partial x^1} + \frac{\partial \Delta T^{22}}{\partial x^2} + (3\Gamma^2_{12} + \Gamma^1_{11})\Delta T^{12} - b^2_2 \Delta T^{23}$$

$$= \gamma h\Bigg(-\omega^2 \frac{\Delta u_2}{a_{22}} + 2\omega \frac{\Delta \dot{u}_1}{\sqrt{a_{11}a_{22}}} \sin\varphi - 2\omega \frac{\Delta \dot{u}_3}{\sqrt{a_{22}}} \cos\varphi + \frac{\Delta \ddot{u}_2}{a_{22}}$$

$$- \omega^2 r\cos\varphi \frac{\Delta\vartheta_2}{a_{22}} \Bigg),$$

$$\frac{\partial \Delta T^{13}}{\partial x^1} + \frac{\partial \Delta T^{23}}{\partial x^2} + (\Gamma^2_{12} + \Gamma^1_{11})\Delta T^{13} + b_{11}\Delta T^{11} + \Delta b_{11} T^{11}_0 + b_{22}\Delta T^{22} + \Delta b_{22} T^{22}_0$$

$$= \gamma h\Bigg[-\omega^2 r \sin\varphi \frac{\Delta\vartheta_1}{\sqrt{a_{11}}} + 2\omega_0\omega r \sin(\omega t + x^2)\sin\varphi + \omega^2 \frac{\Delta u_1}{\sqrt{a_{11}}} \cos\varphi\sin\varphi$$

$$- \omega^2 \Delta u_3 \cos^2\varphi + 2\omega \frac{\Delta \dot{u}_2}{\sqrt{a_{22}}} \cos\varphi + \Delta \ddot{u}_3 \Bigg]. \tag{13}$$

The equations are complemented by equalities (8)–(11) appropriately linearized. They are closed by corresponding boundary conditions.

4. THE PROBLEM SOLUTION TECHNIQUE

The principal peculiarity of system (13) lies in the existence of the multipliers $\sin(\omega t + x^2)$ in their right members, which are associated with inertia loads being harmonic with respect to x^2 and t and running in the circumferential direction with the angular velocity ω and exciting precession vibrations with the frequency ω. This circumstance permits one to represent the even and odd functions of the circumferential co-ordinate x^2 in the form

$$\Delta T^{11}(x^1, x^2, t) = T^{(11)}(x^1)\sin(\omega t + x^2), \quad \Delta T^{(22)}(x^1, x^2, t) = T^{(22)}(x^1)\sin(\omega t + x^2),$$

$$\Delta T^{12}(x^1, x^2, t) = T^{(12)}(x^1)\cos(\omega t + x^2), \quad \Delta T^{13}(x^1, x^2, t) = T^{(13)}(x^1)\sin(\omega t + x^2),$$

$$\Delta T^{23}(x^1, x^2, t) = T^{(23)}(x^1)\cos(\omega t + x^2), \quad \Delta M^{(11)}(x^1, x^2, t) = M^{(11)}(x^1)\sin(\omega t + x^2),$$

$$\Delta M^{22}(x^1, x^2, t) = M^{(22)}(x^1)\sin(\omega t + x^2), \quad \Delta M^{12}(x^1, x^2, t) = M^{(12)}(x^1)\cos(\omega t + x^2),$$

$$\vdots$$

$$\Delta u_1(x^1, x^2, t) = u_{(1)}(x^1)\sin(\omega t + x^2), \quad \Delta u_2(x^1, x^2, t) = u_{(2)}(x^1)\cos(\omega t + x^2),$$

$$\Delta u_3(x^1, x^2, t) = u_{(3)}(x^1)\sin(\omega t + x^2). \tag{14}$$

When expressions (14) are substituted into equation (13) and the multipliers $\sin(\omega t + x^2)$, $\cos(\omega t + x^2)$ are cancelled, the system of eight ordinary differential equations results with x^1 being an independent variable. It can be represented in the form

$$d\mathbf{y}/dx = \mathbf{F}(x)\mathbf{y} + \mathbf{f}(x)\omega_0, \tag{15}$$

where $\mathbf{y} = \{u_{(1)}, u_{(2)}, u_{(3)}, \varepsilon_{(11)}, \varepsilon_{(12)}, \vartheta_{(1)}, \mu_{(11)}, T^{(13)}\}^{\mathrm{T}}$ is the vector of unknown variables; $\mathbf{F}(x)$, $\mathbf{f}(x)$ the certain matrix function and vector function, respectively; $x \equiv x^1$.

System (15) is complemented with appropriate boundary conditions. Its solution is attained with the help of the transfer matrix method. The matrix element functions representing particular solutions of system (15) are constructed by the Runge–Kutta fourth order method. Inasmuch as some summands of the matrix $\mathbf{F}(x)$ elements have large multipliers ω^2, system (15) is rigid and there are fast-growing functions among its particular solutions. For this reason, the method of orthogonalization is used additionally in its numerical integration.

5. RESULTS AND THEIR DISCUSSION

The software created on the basis of the elaborated technique was used for the investigation of dynamics of elastic thin-wall rotor models in compound rotation. First, we consider the simplest ones involving single disks and conic shells. It is established that compound rotation of an elastic disk with free outer edge and clamped by its internal boundary edge to a spinning shaft is not accompanied by resonant regimes of its precession vibrations. Inasmuch as the field of periodically changing displacements $u_{(3)}(x^1, x^2, t)$ depends on the phase co-ordinate $(\omega t + x^2)$ in accord with the harmonic law (14), the vibration mode has the shape of a harmonic wave running in the circumferential direction x^2 with the angular velocity ω, in opposition to the disk spinning. So in the inertial reference frame the vibrations show up as a stagnant harmonic wave, symmetric relative to the plane containing the axes of rotation and slew with maximum displacements located in this plane. In the plane of the spinning axis slewing the normal displacements equal zero.

Figure 2 presents the amplitude of the outer edge deflection $u_{(3)}(x^1 = D/2)$ as a function of the spinning rate ω of a steel disk in the case of its parameters values as follows: the disk internal and external diameters $d = 0{\cdot}24\,\mathrm{m}$, $D = 0{\cdot}8\,\mathrm{m}$; its thickness $h = 0{\cdot}003\,\mathrm{m}$; the disk axis slewing angular velocity $\omega_0 = 1\,\mathrm{s}^{-1}$.

Referring to the figure, one can see that the vibration amplitude grows up to the maximum value and then begins to approach the abscissa axis $0\omega_0$. It can be explained by the fact that the inertia gyro force intensity $2\omega\omega_0 r$ increases proportionally to the first power of ω, whereas the disk bending stiffness caused by its tension with the radial inertial forces depends on the second power of the velocity.

The phenomenon is typical for all other similar disks. It confirms to the Den–Hartog conclusion [5] that even vibrations of a segment of a flexible chain of links in compound rotation do not achieve resonant regimes, not to mention elastic beams and disks which possess relatively higher stiffness.

The situation changes if the internal boundary of an annular disk is free and its external edge is clamped. In this case, the disk spinning gives rise to initiation of compressive internal forces and decrease of its bending stiffness and free vibration frequencies. As a result, a sequence of resonances separated by approximately equal segments $\Delta\omega_j = \omega_{j+1} - \omega_j$ in ω may occur (Figure 3).

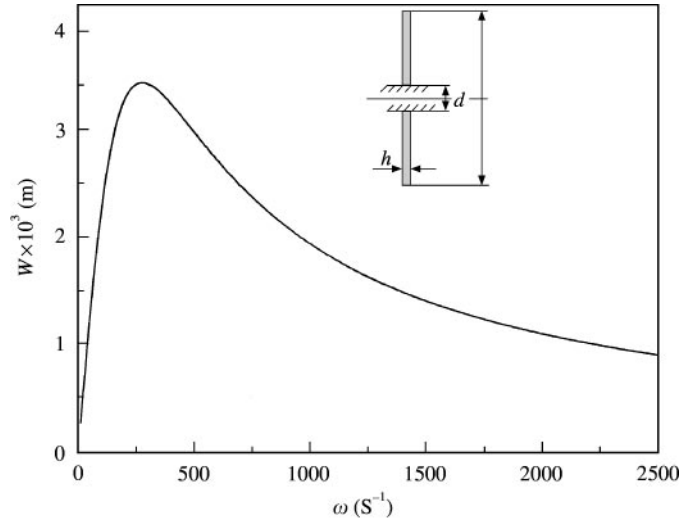

Figure 2. Amplitude of the disk edge precession vibrations versus angular velocity ω.

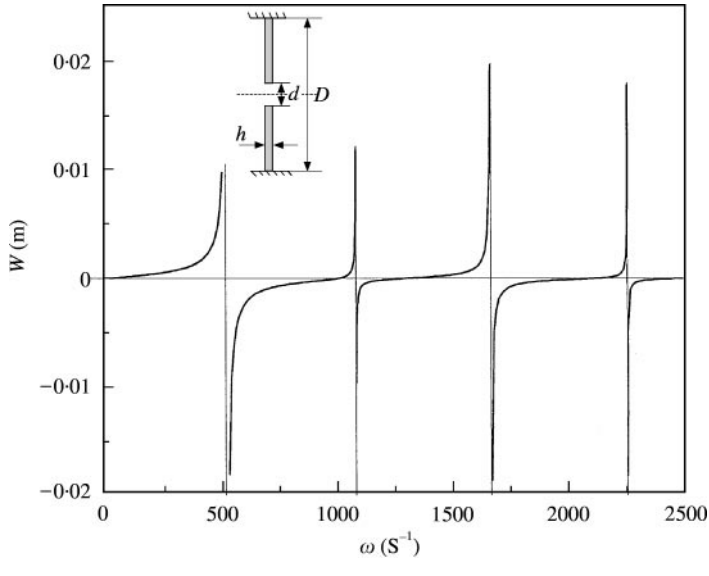

Figure 3. Amplitude of the disk inner edge precession vibrations versus angular velocity ω.

It is known that a gyroscopic moment $\mathbf{M}_g$ is an integral measure of a mechanical system dynamical behaviour in compound rotation. Thus, display of this moment for a rotating axisymmetrical solid body whose axis performs additional compulsory slewing consists in the generation of the body supports reactions making a force couple with the moment

$$\mathbf{M}_g = I_z \boldsymbol{\omega} \times \boldsymbol{\omega}_0. \tag{16}$$

Here I_z is the body moment of inertia relative to the rotation axis.

At the same time the elastic vibrations of a real thin-wall rotor excited by compound rotation are accompanied by the generation of a system of distributed edge elastic bending

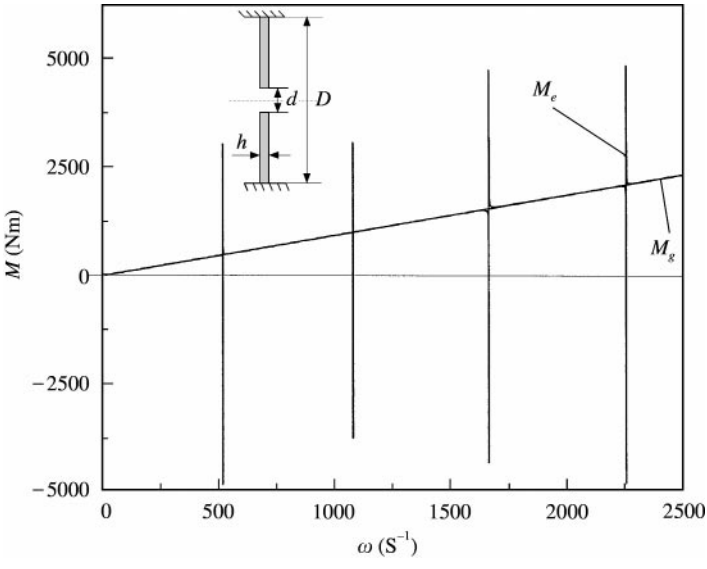

Figure 4. Values of the elastic (M_e) and gyroscopic (M_g) moments in the disk.

TABLE 1

Values of the first resonant angular velocities for the annular disk

	d/D						
D (m)	0·3	0·4	0·45	0·5	0·55	0·6	0·7
1	$332\,s^{-1}$	$286\,s^{-1}$	$271\,s^{-1}$	$266\,s^{-1}$	$273\,s^{-1}$	$292\,s^{-1}$	$384\,s^{-1}$
0·8	$519\,s^{-1}$	$447\,s^{-1}$	$424\,s^{-1}$	$416\,s^{-1}$	$426\,s^{-1}$	$456\,s^{-1}$	$600\,s^{-1}$
0·4	$2078\,s^{-1}$	$1790\,s^{-1}$	$1696\,s^{-1}$	$1665\,s^{-1}$	$1704\,s^{-1}$	$1822\,s^{-1}$	$2399\,s^{-1}$

moments, torques, longitudinal and shear forces applied to the solid spinning carrier and producing a total resultant elastic moment $\mathbf{M}_e$.

In Figure 4 the moduli of the moments $M_e = \pi(D^2 T^*_{(13)}/4 + DM^*_{(1)}/2)$ and $M_g = I_z\omega\omega_0$ are shown, where $T^*_{(13)}$, $M^*_{(1)}$ are the amplitude values of physical components of the internal shear force and bending moment at $x^1 = D/2$. It should be noted that outside the resonant zones which are very narrow, the moments M_g and M_e practically coincide. The calculations were performed for the given values $d = 0{\cdot}24\,\text{m}$, $D = 0{\cdot}8\,\text{m}$, $h = 0{\cdot}003\,\text{m}$.

As the calculations testify, the first resonant values of the considered disk rotation velocity ω_r depend on the dimension of its circular hole. A series of tasks for different parameters d/D and D was solved. In Table 1 the first resonant values of the velocity ω are listed. It can be seen that the minimal values are achieved at the ratio $d/D = 0{\cdot}5$.

The cases discussed above are comparatively straightforward because the state of a simple spinning disk is characterized by a distribution of the centrifugal inertia forces in its plane. For this reason its stress–strain state is planar, where the disk is either stretched or compressed depending on clamping internal or external edge. Additionally, slewing the

rotation axis leads to the generation of precessing inertia forces, normal to its surface, which excite the transverse precession vibrations accompanied by its out-of-plane bending. However, as this takes place, the Coriolis acceleration $\mathbf{a}_c = 0$, since the relative velocity vector $\dot{\mathbf{u}}_3$ is parallel to the rotation axis.

In the general case, when a shell executes compound rotation, all the above-mentioned effects take place and the shell motion is more complicated. As an example consider the compound rotation of a steel conic shell with its small edge clamped and large edge free. The shell parameters are selected as follows: the small edge diameter $d = 0{\cdot}24$ m, the generatrix length $L = 0{\cdot}28$ m, the thickness $h = 0{\cdot}003$ m, and the cone angle 2α was changed inside the limits $0 \leqslant 2\alpha \leqslant 178^\circ$.

The calculations testify that if the angle α is comparatively small the shell does not endure resonant vibrations inside the considered range of ω and the resonant vibration of the selected shell occurs for the angle values $150 \leqslant 2\alpha \leqslant 176^\circ$. In Figure 5 the elastic (M_e) and gyroscopic (M_g) moments are shown as functions of ω for the case $2\alpha = 172^\circ$. The moments practically coincide outside the resonant zones.

To establish the area of plausibility of the obtained results, the computer and experimental simulation of precession vibrations of a spherical segment clamped in its apex was performed. As the preliminary calculations testify, in the cases of not very thin spherical segments ($R/h < 100$) the regimes of the precession resonances are achieved at relatively high values of the rotation rate ω. Inasmuch as experimental investigations of the motion of fast-rotating structures are connected with the essential complication of their performance technique conditioned by stringent demands on the whole system dynamic balancing, considerable increase of the aerodynamical forces and requirements of trouble-free fulfilment, very thin spherical segments ($R/h \approx 1295$) were selected for the experimental investigations. The shell parameters included the following: the curvature radius $R = 123$ mm, the segment base diameter $D = 203$ mm, the thickness $h = 0{\cdot}095$ mm. The shell material density $\gamma = 7{\cdot}8 \times 10^3$ kg/m^3, its elasticity modulus $E = 2{\cdot}1 \times 10^{11}$ Pa, the Poisson coefficient $\nu = 0{\cdot}3$. The diameter of the hole, by which the shell was fixed to the electric motor shaft, measured 9, 12 and 14 mm. The motor shaft rotated with the rate ω, the platform on which the motor was installed slewed with the rate ω_0 around the vertical axis.

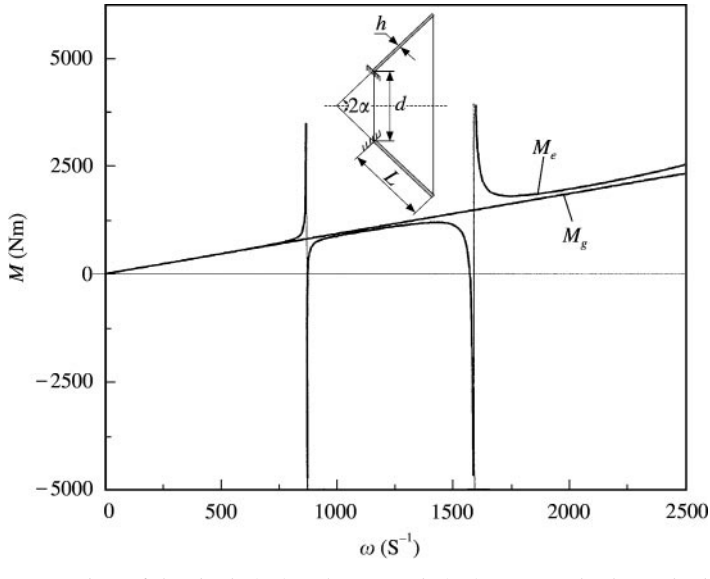

Figure 5. Values of the elastic (M_e) and gyroscopic (M_g) moments in the conic shell.

Owing to the condition $\omega \gg \omega_0$, the precession vibrations quickly assumed stationary mode in the reference frame fixed to the slewing platform.

The shell deflections had the maximal values at the free edge in the planar cross-section containing both the vectors $\boldsymbol{\omega}$, $\boldsymbol{\omega}_0$.

It was found by the calculations and experiments that the fast rotation of the spherical segment pre-stressed it by the centrifugal inertia forces and made it stiffer. However, the additional slewing of its rotation axis led to the essential increment of the internal moments in the vicinity of the clamped edge which increased very fast as the resonant angular velocity ω_r was approached. So it was not possible for the selected thin shells to reach the resonant vibrations because as ω_r was approached the compressed zone of the thin shell buckled near its clamped edge and the formed dent was displaced in the direction opposite to the shell rotation. In the reference frame fixed in the platform, the dent showed up to be immovable. As a consequence of this buckling, the shell surface endured substantial transformation and the shell was quickly destroyed.

In Table 2 are listed the values of calculated resonant rates ω_r and critical rates ω_{cr} established experimentally for the selected values of the clamped edge diameter d and slewing velocity ω_0. It can be seen that the higher the diameter d and the more rigid the shell is, the earlier the shell buckles and the greater is the difference between ω_{cr} and ω_r. Figure 6

TABLE 2

Values of the first resonant and critical angular velocities for the spherical shell

	d (mm)	ω_r (rad/s)	ω_0 (rad/s)	ω_{cr} (rad/s)
1	9	461	0·289	448
2	12	698	0·414	591
3	12	698	0·440	582
4	14	892	0·596	702
5	14	892	0·691	691

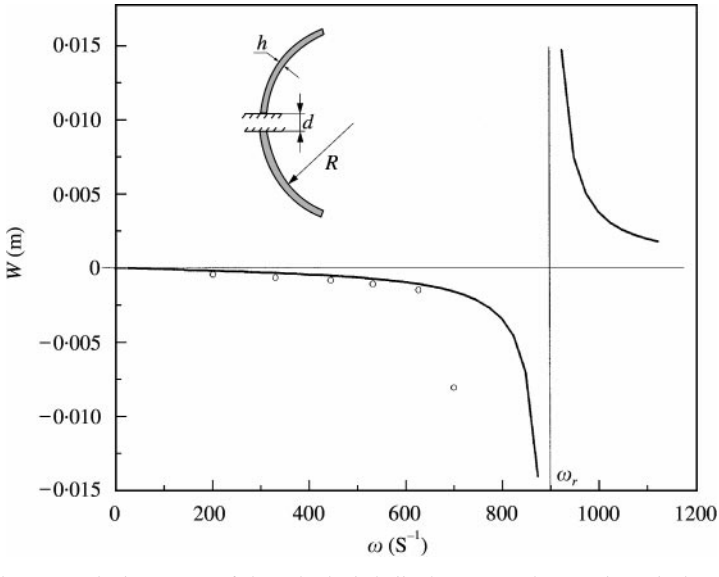

Figure 6. Displacements of the spherical shell edge versus the angular velocity ω.

shows the ω-dependence of the deflection amplitudes of the shell edge for case 5 in Table 2. The solid line represents the calculation results, the circles display the experimental data. Yet it should be underlined that the buckling phenomenon and destruction are typical for very thin shells and thicker shells may behave in another way. In addition, in the comparison the aerodynamical forces playing an important role at high values of ω were not taken into account.

6. CONCLUSIONS

The obtained results of numerical and experimental investigations enable one to draw the following inferences.

1. The compound rotation of thin elastic disks and shells is accompanied by generation of their precession vibrations in the mode of a running harmonic wave, which in the inertial reference frame shows up as a stationary deformed surface symmetric relative to the plane containing both the vectors of the angular velocities of the rotation and slewing.
2. It is established theoretically that the resonant vibrational regimes may occur in compound rotation of annular disks clamped by their outer edge and conical and spherical shells. Compound rotation of thin disks clamped by their inner boundary is not accompanied by the resonant vibrations.
3. It is established experimentally that the extremely thin spherical shells ($R/h \approx 1300$) buckle and are quickly destroyed near the clamped inner edge in the vicinity of the resonant values ω_r predicted theoretically.

REFERENCES

1. N. E. EGARMIN 1986 *Mechanics of Solids* **21**, 142–148. On precession of steady waves of rotating axisymmetrical shell vibrations (in Russian).
2. J. PADOVAN 1973 *Journal of Sound and Vibration* **31**, 469–482. Natural frequencies of rotating pre-stressed cylinders.
3. K. R. SIVADAS 1995 *Journal of Sound and Vibration* **186**, 99–109. Vibration analysis of pre-stressed rotating thick circular conical shell.
4. A. L. SMIRNOV and P. E. TOVSTIK 1982 (M. A. Laurentjev, editor) In: *Modern Problems of Mechanics and Aviation* 280–290. Moscow: Mashinostrojenie. Qualitative investigation of dynamics of rotating axisymmetrical shells (in Russian).
5. V. I. GULYAYEV and P. P. LIZUNOV 1989 *Vibrations of Systems of Solid and Deformarble Bodies in Compound Motion*. Kiev: Vyshcha Shkola (in Russian).
6. V. I. GULYAYEV and R. V. DOMARETSKY 1996 *Strength of Materials* **N6**, 71–81. Vibrations of elastic bladed disk in compound rotation (in Russian).
7. A. I. LURIE 1961 *Analytical Mechanics*. Moscow: Nauka (in Russian).
8. V. I. GULYAYEV, V. A. BAZHENOV and E. A. GOTSULIAK 1983 *Stability of Periodical Processes in Non-linear Mechanical Systems*. L'vov: Vyshcha Shkola (in Russian).